# Characterization of a Multicomponent Alkyl Methacrylate Copolymer by High-Resolution Pyrolysis–Gas Chromatography

**Hajime Ohtani, Takaaki Asai, and Shin Tsuge***

*Department of Synthetic Chemistry, Faculty of Engineering, Nagoya University, Nagoya 464, Japan.* *Received August 14, 1984*

ABSTRACT: Pyrolysis–fused silica capillary gas chromatography (PyGC) was successfully applied to determining the composition and the isomer distribution of a complex alkyl methacrylate copolymer. The characteristic peaks on the pyrogram were almost completely separated from each other. The peak identification was primarily carried out by a directly coupled PyGC–MS system, while the pyrolysis–hydrogenation technique was additionally applied to determine the exact carbon skeleton of the monomers. The copolymer proved to be composed of more than 20 components of methacrylates associated with $C_1$, $C_{12}$–$C_{16}$, and $C_{18}$ alcohols. The distributions of the monomeric isomers were also determined with excellent reproducibility.

Polymethacrylates are widely used in the field of plastics, paints, and binders for ceramics. In addition, alkyl methacrylate copolymers are also used as viscosity index (VI) improvers for lubricating oils. Such polymethacrylates are usually synthesized through copolymerization of a monomer mixture of methacrylic acid esters with $C_1$–$C_{30}$ alcohols including various branched isomers. The properties of the VI improvers are strongly affected not only by the composition but also by the type and the degree of branching of the associated alcohols. However, the whole compositional analysis of such multicomponent copolymers has been difficult even by IR and NMR.

On the other hand, pyrolysis–gas chromatography (PyGC) has often been employed for the characterization of alkyl methacrylate copolymers. Guillet et al.[1] applied PyGC to the quantitative analysis of copolymers of butyl and hexyl methacrylate. VI improvers of polymethacrylates were analyzed by Sugiura et al.[2] and by Kempe et al.[3] However, the results were limited to determination of the main monomeric constituents primarily because of insufficient peak separation by conventional packed columns.

In this work, PyGC technique was improved by incorporating a fused-silica capillary column to obtain high-resolution pyrograms of such a multicomponent copolymer as a VI improver. Pyrolysis–hydrogenation technique was also effectively utilized to determine the carbon skeleton of the monomeric constituents. On the basis of the observed high-resolution pyrograms of a commercial VI improver, thermal degradation behaviors of polymethacrylates were first examined, and then determination of the composition and the isomer distribution was carried out with excellent reproducibility.

## Experimental Section

**Samples.** A commercial lubricating oil additive utilized as a VI improver, which consists of 60–70% of alkyl methacrylate copolymers and the rest of hydrocarbon base oil with a flash point of 200 °C, was subjected to the analysis. The polymer fraction was isolated from the matrix by dissolving the original material in pentane followed by precipitating with a mixture solvent of methanol and 2-propanol. The precipitate was dried in vacuo at 150 °C for 20 min. The number-averaged molecular weight of the polymer was $2.8 \times 10^4$, and the heterogeneity index $M_w/M_n$ was 1.8. As a reference polymer for PyHGC work, an ethylene–propylene copolymer (P(E-P)) containing 13.1 wt % of propylene was used.

**Conditions for PyGC.** A vertical microfurnace-type pyrolyzer (Yanagimoto GP-1018) was directly attached to a gas chromatograph (Shimadzu-7AG) with a fused-silica capillary column (0.32-mm o.d. × 0.2-mm i.d. × 30 m long) coated with immobilized OV-1 through chemical cross-linking supplied by Hewlett-Packard. The 50 mL min$^{-1}$ carrier gas flow at the pyrolyzer was reduced to 0.7 mL min$^{-1}$ at the capillary column by a splitter. For conventional PyGC measurement, nitrogen was used as the carrier gas. On the other hand, for pyrolysis–hydrogenation gas chromatography (PyHGC), hydrogen carrier gas was used together with a hydrogenation catalyst column[4] (3-mm i.d. × 10 cm long) containing 5 wt % of Pt packing (80–100 mesh Diasolid H) which was inserted in series between the pyrolyzer and a splitter, and maintained at 200 °C. The column temperature was programmed from 70 to 280 °C at a rate of 3 °C min$^{-1}$ for conventional PGC and 2 °C min$^{-1}$ for PyHGC. A sample size of about 80 μg was pyrolyzed under the flow of carrier gas. A directly coupled gas chromatograph–mass spectrometer (JEOL JMS-DX300) was used for peak identification.

## Results and Discussion

**Peak Assignment of the Pyrograms and Thermal Behaviors of the Copolymer.** It is known that polymethacrylates depolymerize to give nearly quantitative yields of the corresponding monomers when heated above a certain "threshold" temperature. In order to perform rapid thermal degradation, higher pyrolysis temperatures are generally desirable. At the elevated temperatures, however, secondary degradation of the primary products becomes significant. In this work, various pyrolysis temperatures between 400 and 750 °C were examined.

Figure 1 shows the pyrograms of the alkyl methacrylate copolymer at 450 (A), 600 (B), and 700 (C) °C. At 450 °C, the pyrogram mostly consists of the associated alkyl methacrylate monomers (ca. 97%) with minor olefinic products (ca. 3%), at 600 °C the peak intensities of the monomers and the olefins become comparable with each other, and finally at 700 °C the monomer peaks disappear except for that of methyl methacrylate (MMA) and instead the strong olefinic peaks are observed along with additional lower boiling point fragments at the earlier retention times. The olefinic products are formed together with methacrylic acid,[5] for example from the depolymerized straight-chained monomer through further thermal degradation:

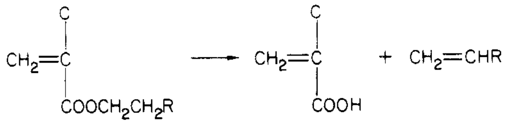

$$CH_2{=}C(C)COOCH_2CH_2R \longrightarrow CH_2{=}C(C)COOH + CH_2{=}CHR$$

(R: alkyl group)

A skewed peak of methacrylic acid is observed just after the peak of MMA at the higher pyrolysis temperatures.

Most of the peaks on the pyrograms were identified by the directly coupled PyGC-MS. In this work, however, the PyHGC method was also supplementally applied to determine the exact carbon skeleton of the monomers. This technique provides a simplified pyroram through in-line hydrogenation of the degradation products into the asso-

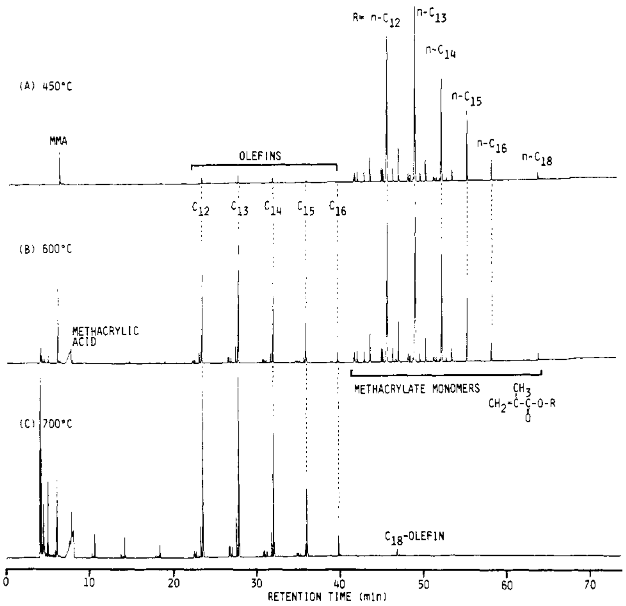

**Figure 1.** Pyrograms of the alkyl methacrylate copolymer: A) at 450 °C, (B) at 600 °C, (C) at 700 °C.

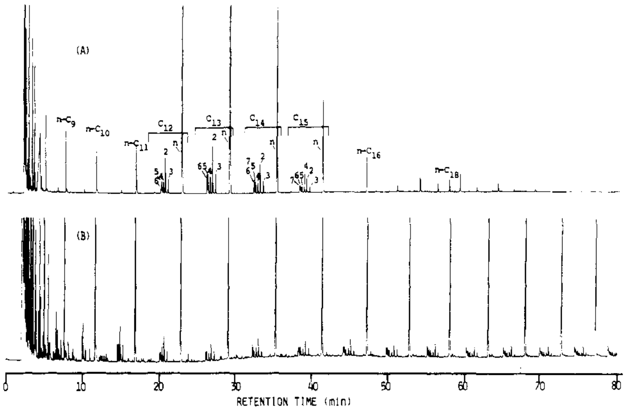

**Figure 2.** Hydrogenated pyrograms at 720 °C: (A) the alkyl methacrylate copolymer; (B) ethylene–propylene copolymer (propylene 13.1 wt %). 7 = 7-methylparaffin; 6 = 6-methylparaffin; 5 = 5-methylparaffin; 4 = 4-methylparaffin; 3 = 3-methylparaffin; 2 = 2-methylparaffin; $n$ = $n$-paraffin.

ciated paraffins which reflect only the carbon skeleton of the original products. The hydrogenated pyrogram of the copolymer sample at 720 °C is shown in Figure 2 along with that of the reference ethylene–propylene copolymer (P(E-P)). Besides the main peaks of $n$-paraffins, various isoparaffins are also observed for $C_{12}$–$C_{15}$.

It is very interesting to note that the observed pattern of the isoparaffin peaks for each carbon number is almost identical with that of the reference model copolymer whose microstructures are well characterized by PyHGC.[6,7] Thus identified every isoparaffin peak on the pyrogram of the polymethacrylate sample has one methyl branch. The number on the pyrogram in Figure 2A indicates the position of the methyl branch in the molecule. For example, 2 and 3 in the $C_{12}$ region represent 2-methylundecane and 3-methylundecane, respectively. These data suggest that the raw alcohols for the $C_{12}$–$C_{15}$ methacrylate monomers should have the following structure:

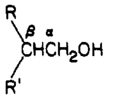

$RR'CHCH_2OH$ (R, R': alkyl group or hydrogen)

This observation reveals that the raw alcohols are synthesized through hydroformylation of olefins followed by hydrogenation. Accordingly the branching in the monomers always exists at the $\beta$ position.

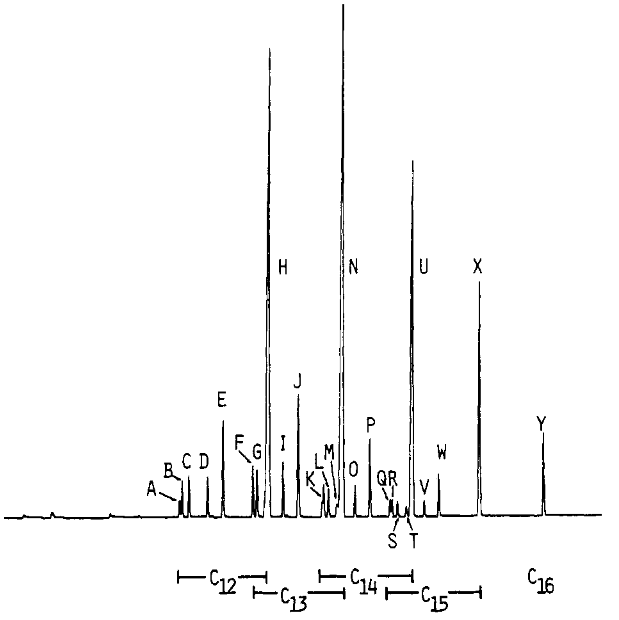

**Figure 3.** Detailed pyrogram of the alkyl methacrylate copolymer at 450 °C for $C_{12}$–$C_{16}$ methacrylates. A–Y are assigned in Table I.

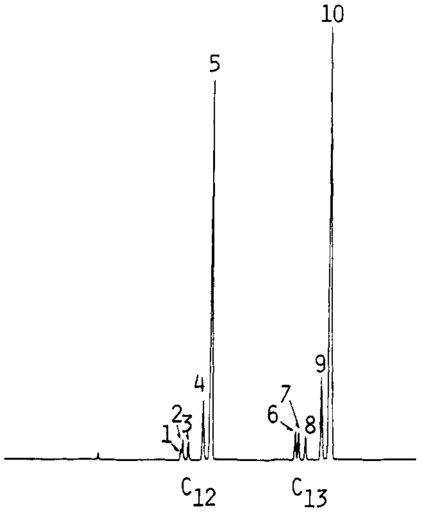

**Figure 4.** Expanded pyrogram of the alkyl methacrylate copolymer at 600 °C for $C_{12}$ and $C_{13}$ olefin region. Peak assignments are listed in Table II.

Table I summarizes the assigned peaks of the monomers on the pyrogram shown in Figure 3 (a detailed partial pyrogram of Figure 1A). Almost complete separation is attained except for peaks H and K; the former contains dodecyl methacrylate ($n$-$C_{12}$(M)) and 2-propyldecyl methacrylate (2P-$C_{13}$(M)), and the latter 2-hexyloctyl methacrylate (2H-$C_{14}$(M)) and 2-amylnonyl methacrylate (2A-$C_{14}$(M)), respectively.

Table II lists the identified olefinic products on the detailed pyrogram of Figure 4 for the $C_{12}$ and $C_{13}$ regions (a detailed partial pyrogram of Figure 1B). It should be noted that the peaks of straight-chained ($n$) and ethyl-branched (2E) products are always overlapping with each other for the olefins of any carbon number.

As can be seen from the data in Tables I and II, most of the characteristic peaks on the pyrograms are separated from each other with some exceptions. However, the fact that the olefinic components associated with the overlapped monomer peaks are resolved on the same pyrogram

Table I
Peak Assignments of the Monomers

| peak no.[a] | peak assignment | structure of R[b] |
|---|---|---|
| A | 2-amylheptyl methacrylate (2A-$C_{12}$(M)) | 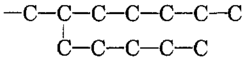 $-C-\underset{C-C-C-C-C}{\underset{\vert}{C}}-C-C-C-C-C$ |
| B | 2-butyloctyl methacrylate (2B-$C_{12}$(M)) | 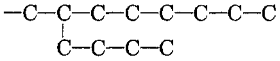 $-C-\underset{C-C-C-C}{\underset{\vert}{C}}-C-C-C-C-C-C$ |
| C | 2-propylnonyl methacrylate (2P-$C_{12}$(M)) | 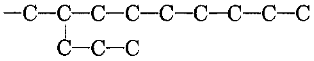 $-C-\underset{C-C-C}{\underset{\vert}{C}}-C-C-C-C-C-C-C$ |
| D | 2-ethyldecyl methacrylate (2E-$C_{12}$(M)) | 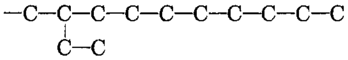 $-C-\underset{C-C}{\underset{\vert}{C}}-C-C-C-C-C-C-C-C$ |
| E | 2-methylundecyl methacrylate (2M-$C_{12}$(M)) | 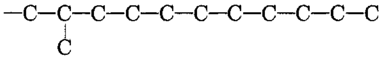 $-C-\underset{C}{\underset{\vert}{C}}-C-C-C-C-C-C-C-C-C$ |
| F | 2-amyloctyl methacrylate (2A-$C_{13}$(M)) | 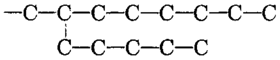 $-C-\underset{C-C-C-C-C}{\underset{\vert}{C}}-C-C-C-C-C-C$ |
| G | 2-butylnonyl methacrylate (2B-$C_{13}$(M)) | 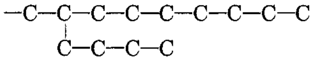 $-C-\underset{C-C-C-C}{\underset{\vert}{C}}-C-C-C-C-C-C-C$ |
| H | 2-propyldecyl methacrylate (2P-$C_{13}$(M)) | 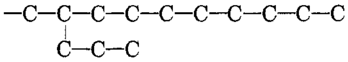 $-C-\underset{C-C-C}{\underset{\vert}{C}}-C-C-C-C-C-C-C-C$ |
|  | dodecyl methacrylate (*n*-$C_{12}$(M)) | —C—C—C—C—C—C—C—C—C—C—C—C |
| I | 2-ethylundecyl methacrylate (2E-$C_{13}$(M)) | 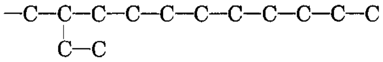 $-C-\underset{C-C}{\underset{\vert}{C}}-C-C-C-C-C-C-C-C-C$ |
| J | 2-methyldodecyl methacrylate (2M-$C_{13}$(M)) | 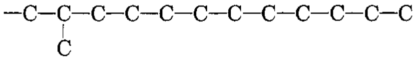 $-C-\underset{C}{\underset{\vert}{C}}-C-C-C-C-C-C-C-C-C-C$ |
| K | 2-hexyloctyl methacrylate (2H-$C_{14}$(M)) | 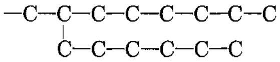 $-C-\underset{C-C-C-C-C-C}{\underset{\vert}{C}}-C-C-C-C-C-C$ |
|  | 2-amylnonyl methacrylate (2A-$C_{14}$(M)) | 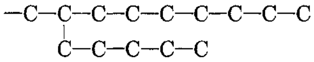 $-C-\underset{C-C-C-C-C}{\underset{\vert}{C}}-C-C-C-C-C-C-C$ |
| L | 2-butyldecyl methacrylate (2B-$C_{14}$(M)) | 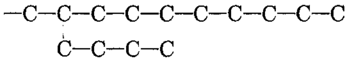 $-C-\underset{C-C-C-C}{\underset{\vert}{C}}-C-C-C-C-C-C-C-C$ |
| M | 2-propylundecyl methacrylate (2P-$C_{14}$(M)) | 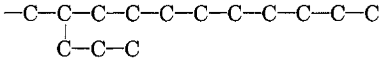 $-C-\underset{C-C-C}{\underset{\vert}{C}}-C-C-C-C-C-C-C-C-C$ |
| N | tridecyl methacrylate (*n*-$C_{13}$(M)) | —C—C—C—C—C—C—C—C—C—C—C—C—C |
| O | 2-ethyldodecyl methacrylate (2E-$C_{14}$(M)) | 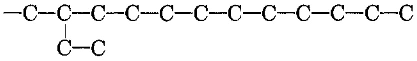 $-C-\underset{C-C}{\underset{\vert}{C}}-C-C-C-C-C-C-C-C-C-C$ |
| P | 2-methyltridecyl methacrylate (2M-$C_{14}$(M)) | 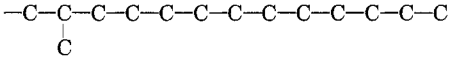 $-C-\underset{C}{\underset{\vert}{C}}-C-C-C-C-C-C-C-C-C-C-C$ |
| Q | 2-hexylnonyl methacrylate (2H-$C_{15}$(M)) | 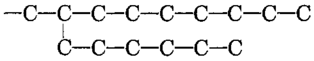 $-C-\underset{C-C-C-C-C-C}{\underset{\vert}{C}}-C-C-C-C-C-C-C$ |
| R | 2-amyldecyl methacrylate (2A-$C_{15}$(M)) | 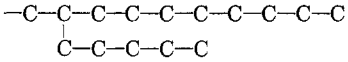 $-C-\underset{C-C-C-C-C}{\underset{\vert}{C}}-C-C-C-C-C-C-C-C$ |
| S | 2-butylundecyl methacrylate (2B-$C_{15}$(M)) | 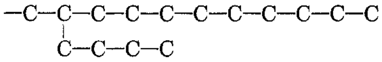 $-C-\underset{C-C-C-C}{\underset{\vert}{C}}-C-C-C-C-C-C-C-C-C$ |
| T | 2-propyldodecyl methacrylate (2P-$C_{15}$(M)) | 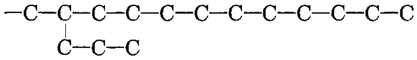 $-C-\underset{C-C-C}{\underset{\vert}{C}}-C-C-C-C-C-C-C-C-C-C$ |
| U | tetradecyl methacrylate (*n*-$C_{14}$(M)) | —C—C—C—C—C—C—C—C—C—C—C—C—C—C |
| V | 2-ethyltridecyl methacrylate (2E-$C_{15}$(M)) | 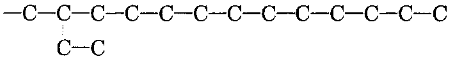 $-C-\underset{C-C}{\underset{\vert}{C}}-C-C-C-C-C-C-C-C-C-C-C$ |
| W | 2-methyltetradecyl methacrylate (2M-$C_{15}$(M)) | 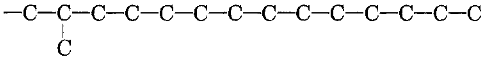 $-C-\underset{C}{\underset{\vert}{C}}-C-C-C-C-C-C-C-C-C-C-C-C$ |
| X | pentadecyl methacrylate (*n*-$C_{15}$(M)) | —C—C—C—C—C—C—C—C—C—C—C—C—C—C—C |
| Y | hexadecyl methacrylate (*n*-$C_{16}$(M)) | —C—C—C—C—C—C—C—C—C—C—C—C—C—C—C—C |

[a] Peak numbers correspond to those in Figure 3. [b] R for $CH_2{=}C(CH_3)COOR$.

suggests that a complete compositional estimation could be made if the olefinic peaks are also taken into consideration for the determination of the unresolved monomer components. Therefore, the thermal behavior of the methacrylate copolymer was first examined before proceeding to the compositional discussion.

As a typical example, the monomers associated with $C_{15}$ alcohols were examined in detail with respect to the temperature dependence of the monomer recoveries. Figure 5 shows the observed monomer recoveries for the isomers relative to those at 450 °C as a function of the pyrolysis temperature. Although above 600 °C a rapid decrease in the recovery is observed for every monomer, it should be noted that the thermal stabilities for the isomers at the higher pyrolysis temperatures are in the order of 2M > 2E ~ 2P ~ 2B ~ 2A ~ 2H > *n*. The same tendency can be observed for the other isomers with different carbon number.

On the contrary, among the olefinic peaks with the same carbon number formed through the further thermal degradation of the associated monomers, the relative yields are in the order of *n* > 2E ~ 2P ~ 2B ~ 2A ~ 2H > 2M.

Table II
Peak Assignments of $C_{12}$ and $C_{13}$ Olefins

| peak no.[a] | peak assignment | structure |
|---|---|---|
| 1 | 2-amyl-1-heptene (2A-$C_{12}$) | 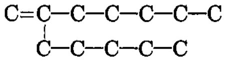 $\begin{array}{l}C{=}C{-}C{-}C{-}C{-}C{-}C\\ \quad\vert\\ \quad C{-}C{-}C{-}C{-}C\end{array}$ |
| 2 | 2-butyl-1-octene (2B-$C_{12}$) | 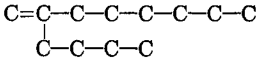 $\begin{array}{l}C{=}C{-}C{-}C{-}C{-}C{-}C{-}C\\ \quad\vert\\ \quad C{-}C{-}C{-}C\end{array}$ |
| 3 | 2-propyl-1-nonene (2P-$C_{12}$) | 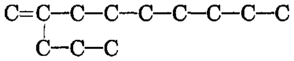 $\begin{array}{l}C{=}C{-}C{-}C{-}C{-}C{-}C{-}C{-}C\\ \quad\vert\\ \quad C{-}C{-}C\end{array}$ |
| 4 | 2-methyl-1-undecene (2M-$C_{12}$) | 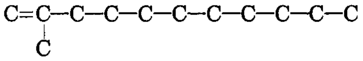 $\begin{array}{l}C{=}C{-}C{-}C{-}C{-}C{-}C{-}C{-}C{-}C{-}C\\ \quad\vert\\ \quad C\end{array}$ |
| 5 | 2-ethyl-1-decene (2E-$C_{12}$) | 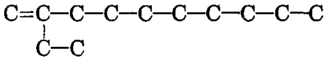 $\begin{array}{l}C{=}C{-}C{-}C{-}C{-}C{-}C{-}C{-}C{-}C\\ \quad\vert\\ \quad C{-}C\end{array}$ |
|  | 1-dodecene ($n$-$C_{12}$) | $C{=}C{-}C{-}C{-}C{-}C{-}C{-}C{-}C{-}C{-}C{-}C$ |
| 6 | 2-amyl-1-octene (2A-$C_{13}$) | 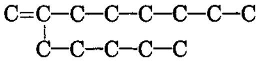 $\begin{array}{l}C{=}C{-}C{-}C{-}C{-}C{-}C{-}C\\ \quad\vert\\ \quad C{-}C{-}C{-}C{-}C\end{array}$ |
| 7 | 2-butyl-1-nonene (2B-$C_{13}$) | 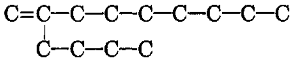 $\begin{array}{l}C{=}C{-}C{-}C{-}C{-}C{-}C{-}C{-}C\\ \quad\vert\\ \quad C{-}C{-}C{-}C\end{array}$ |
| 8 | 2-propyl-1-decene (2P-$C_{13}$) | 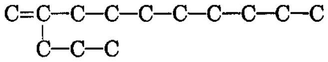 $\begin{array}{l}C{=}C{-}C{-}C{-}C{-}C{-}C{-}C{-}C{-}C\\ \quad\vert\\ \quad C{-}C{-}C\end{array}$ |
| 9 | 2-methyl-1-dodecene (2M-$C_{13}$) | 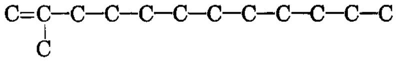 $\begin{array}{l}C{=}C{-}C{-}C{-}C{-}C{-}C{-}C{-}C{-}C{-}C{-}C\\ \quad\vert\\ \quad C\end{array}$ |
| 10 | 2-ethyl-1-undecene (2E-$C_{13}$) | 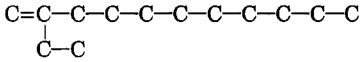 $\begin{array}{l}C{=}C{-}C{-}C{-}C{-}C{-}C{-}C{-}C{-}C{-}C\\ \quad\vert\\ \quad C{-}C\end{array}$ |
|  | 1-tridecene ($n$-$C_{13}$) | $C{=}C{-}C{-}C{-}C{-}C{-}C{-}C{-}C{-}C{-}C{-}C{-}C$ |

[a] Peak numbers correspond to those in Figure 4.

From these data it is obvious that there always exist complementary relations between the recoveries of the monomers and the associated olefins on the same pyrogram measured under given pyrolysis conditions and that the thermal behavior is almost comparable especially for 2E, 2P, 2B, 2A, and 2H isomers.

**Compositional Determination of the Copolymer.** Below 400 °C, an appreciable peak broadening was observed for the fragments with earlier retention times because of the slow thermal degradation of the sample under a flow of carrier gas (50 mL $min^{-1}$). Therefore, for the following compositional analysis, pyrolysis temperatures above 450 °C were used. Peak intensities for the monomers and the associated olefins with a given carbon number with both a straight and a branched alkyl group were collectively evaluated for the determination after making molar sensitivity correction for FID. However, since peak H contains $n$-$C_{12}$(M) and 2P-$C_{13}$(M) fractions, the peak intensity was divided in the following way by using the data of the related olefinic peaks. As mentioned above, the observed thermal stabilities of the methacrylate monomers are in the order of 2M > 2E ~ 2P ~ 2B ~ 2A ~ 2H > $n$. Therefore, the distributions of the monomers and the associated olefins are expected to be complementary and comparable on the same pyrogram among the isomers related with 2E, 2P, 2B, 2A, and 2H. Among these, 2A-$C_{13}$(M) (peak F), 2B-$C_{13}$(M) (peak G), and 2E-$C_{13}$(M) (peak I) are separated from each other for the $C_{13}$-related methacrylate isomers (Table I), while the olefinic 2E-$C_{13}$ is overlapped with that of $n$-$C_{13}$ in peak 10 (Table II). Therefore, in the following calculation 2A-$C_{13}$ and 2B-$C_{13}$ are used as the reference peaks against 2P-$C_{13}$(M)

$$I_m(\text{2P-}C_{13}(\text{M})) = I_m(\text{2A-}C_{13}(\text{M}) + \text{2B-}C_{13}(\text{M}))\frac{I_o(\text{2P-}C_{13})}{I_o(\text{2A-}C_{13} + \text{2B-}C_{13})}$$

$$I_m(n\text{-}C_{12}(\text{M})) = I_m(\text{peak H}) - I_m(\text{2P-}C_{13}(\text{M}))$$

where $I_m$ and $I_o$ represent the peak intensities of the monomers at a given pyrolysis temperature between 450 and 650 °C and that of olefins at 650 °C, respectively. The monomer yield of MMA was assumed to be constant (100%) at any pyrolysis temperature utilized because of its high thermal stability. Table III shows the observed

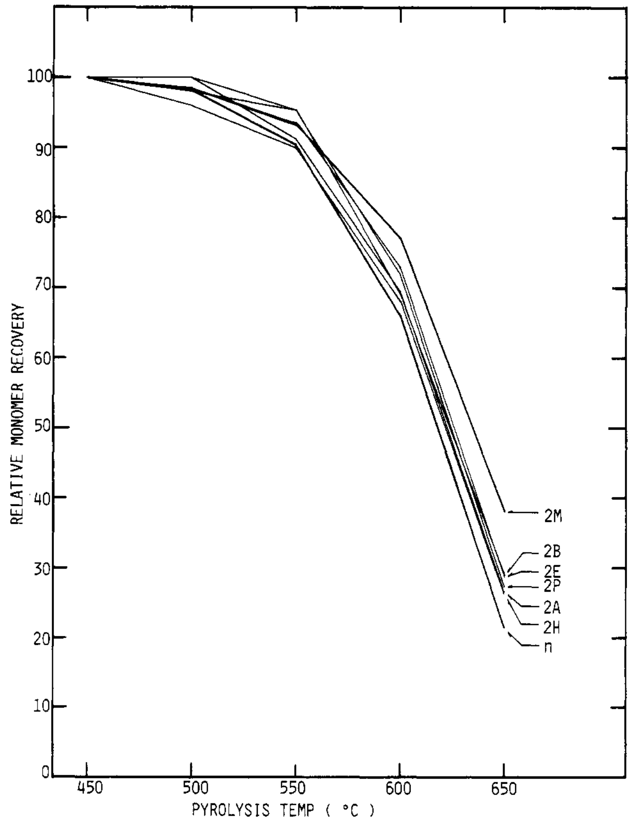

**Figure 5.** Relative recoveries for the isomers of $C_{15}$ methacrylates. Each recovery was normalized in such a way that relative recovery = 100 at 450 °C. 2M = 2-methyltetradecyl methacrylate; 2B = 2-butylundecyl methacrylate; 2E = 2-ethyltridecyl methacrylate; 2P = 2-propyldodecyl methacrylate; 2A = 2-amyldecyl methacrylate; 2H = 2-hexylnonyl methacrylate; $n$ = pentadecyl methacrylate.

**Table III**
**Estimated Composition of the Methacrylate Copolymer**

| | pyrolysis temp, °C | utilized peak | mole fraction in the copolymer,[a] % | | | | | | |
|---|---|---|---|---|---|---|---|---|---|
| | | | $C_1$[b] | $C_{12}$[b] | $C_{13}$[b] | $C_{14}$[b] | $C_{15}$[b] | $C_{16}$[b] | $C_{18}$[b] |
| A | 450 | monomers + olefins | 11.3 (0.7) | 25.7 (0.3) | 33.5 (0.1) | 18.4 (0.1) | 8.9 (0.6) | 1.7 (1.2) | 0.5 (0.6) |
| B | 450 | monomers | 11.7 (0.6) | 25.6 (0.3) | 33.4 (0.1) | 18.3 (0.1) | 8.9 (0.6) | 1.6 (1.2) | 0.5 (1.8) |
| C | 650 | monomers + olefins | 11.9 (1.4) | 25.6 (0.4) | 33.2 (0.5) | 18.2 (0.5) | 9.0 (0.8) | 1.6 (0.9) | 0.5 (1.2) |
| D | 650 | monomers | 35.1 (19.0) | 18.9 (9.9) | 24.6 (10.3) | 12.5 (10.6) | 6.6 (10.2) | 1.1 (12.7) | 0.4 (13.9) |

[a] Values in parentheses are relative standard deviations calculated for five repeated runs (%). [b] Carbon number of R for $CH_2{=}C(CH_3)$-COOR.

**Table IV**
**Estimated Distributions of Isomers among the Monomers with the Same Carbon Number**[a]

| carbon number in R[c] | relative abundance,[b] % | | | | | | |
|---|---|---|---|---|---|---|---|
| | 2H[d] | 2A[d] | 2B[d] | 2P[d] | 2E[d] | 2M[d] | *n*[d] |
| $C_{12}$ | | 1.8 (0.9) | 3.4 (0.4) | 3.9 (0.4) | 3.5 (0.9) | 9.5 (0.6) | 77.9 (0.1) |
| $C_{13}$ | | 3.7 (0.2) | 3.6 (0.3) | 3.2 (0.2) | 3.6 (0.3) | 9.9 (0.2) | 76.0 (0.1) |
| $C_{14}$ | 5.9 (0.2)[e] | | 3.7 (0.8) | 3.0 (9.2) | 3.8 (4.1) | 9.8 (0.5) | 73.8 (0.2) |
| $C_{15}$ | 4.7 (3.0) | 4.0 (3.2) | 4.0 (1.2) | 3.5 (1.5) | 3.7 (1.0) | 10.1 (0.4) | 70.1 (0.1) |

[a] Estimated from relative peak intensities of monomers on the pyrogram at 450 °C. [b] Values in parentheses are relative standard deviations calculated for five repeated runs (%). [c] Carbon number of R for $CH_2{=}C(CH_3)COOR$. [d] Branching of R: 2H = 2-hexyl; 2A = 2-amyl; 2B = 2-butyl; 2P = 2-propyl; 2E = 2-ethyl; 2M = 2-methyl; *n* = normal. [e] Total value for 2H and 2A.

compositional results of the copolymer under various experimental conditions.

At 450 °C about 97 mol % is recovered as the monomers and the rest (3 mol %) is observed as the associated olefins. The compositional results A are obtained by using both the monomers and the olefins. The reproducibility for the analysis is less than 3% of relative standard deviation even for the minor components. However, the values calculated from the monomer data alone (B) are almost comparable with those of A since the contributions of the associated olefins are negligible small at this pyrolysis temperature.

On the other hand, at the elevated pyrolysis temperatures above 450 °C, the contribution of the olefins becomes significant. At 650 °C, when only the monomers are utilized, the resulting compositional values D are remarkably deviated from those of A primarily because of the great difference in the monomer recoveries between MMA and the higher methacrylate, and what is worse, the reproducibility becomes poorer since the secondary thermal reactions to form the olefins from the associated monomers are highly susceptible to the subtle changes in the pyrolysis conditions. However, when both the monomers and the olefins are considered together, the compositional values as well as the reproducibility data C become comparable to those of A since the contributions of the secondary reactions are compensated by considering the associated olefins. Thus, it is possible to perform the compositional analysis of such a complex copolymer at any pyrolysis temperature between 450 and 650 °C provided that both the monomers and the associated olefins are considered together.

Table IV summarizes isomer distributions among the same carbon number methacrylates in the copolymer determined from the relative yields of the isomeric monomers at the pyrolysis temperature of 450 °C. The values for the overlapped peak (peak H in Table I) was separately evaluated by the same way mentioned above. As 2H-$C_{14}$ and 2A-$C_{14}$ are not resolved even in the corresponding olefinic region, their total abundance is given in Table IV. Reproducibility of the results is generally satisfactory. However, the relatively large CV value of 9% for 2P-$C_{14}$(M) should be attributed to its insufficient resolution from *n*-$C_{13}$(M) as shown in Figure 3.

The fact that the distributions of the isomers are comparable with each other for the monomers with different carbon number (70–78% for *n*-, 9.5–10% for 2M-, and 3.0–4.0% for 2E-, 2P-, and 2B-) also suggests that the raw alcohols with $C_{12}$–$C_{15}$ are synthesized through basically the same reactions.

In conclusion, high-resolution PyGC, when combined with PyHGC, is a powerful method to make the whole compositional analysis of a complex copolymer consisting of more than 20 components. Exactly the same method is now currently applied to the characterization of paints, binder polymers for ceramics, and surfactants with various distributions of alkyl groups.

## References and Notes

(1) Guillet, J. E.; Wooten, W. C.; Combs, R. L. *J. Appl. Polym. Sci.* **1960**, *7*, 61.
(2) Sugiura, K.; Tago, S.; Kondo, O.; Sekino, Y. *Sekiyu Gakkaishi* **1970**, *5*, 363.
(3) Kempe, J.; Zimmermann, V. *Schmierungstechnik* **1983**, *14*, 209.
(4) Ohtani, H.; Tsuge, S.; Ogawa, T.; Elias, H.-G. *Macromolecules* **1984**, *17*, 465.
(5) Hewitt, G. C.; Whitham, B. T. *Analyst (London)* **1961**, *86*, 643.
(6) Sugimura, Y.; Tsuge, S. *Macromolecules* **1979**, *12*, 512.
(7) Sugimura, Y.; Usami, T.; Nagaya, T.; Tsuge, S. *Macromolecules* **1981**, *14*, 1787.